Hot–Dog Structured Protective Nanocoating for Multifunctional Cotton Fabric Through Spray Assisted Layer–by–Layer Assembly

Fanxin Zeng
Donghua University College of Materials Science and Engineering
Xian Xu
Donghua University College of Materials Science and Engineering
Yueying Shen
Donghua University College of Materials Science and Engineering
Yeping Liu
Donghua University College of Materials Science and Engineering
Xueshi Shan
Donghua University College of Materials Science and Engineering
Zongyi QIN (phqin@dhu.edu.cn)
Donghua University https://orcid.org/0000-0002-6329-4005

Research Article

Keywords: Multifunctional cotton fabric, Polyaniline nanofibers, Hot–dog structure, Phosphorus–silicon–nitrogen synergism, Spray assisted layer–by–layer assembly

Posted Date: June 17th, 2021

DOI: https://doi.org/10.21203/rs.3.rs-275022/v1

Abstract

Multifunctional cotton fabric was preparation by low–cost and environmental–friendly spray–assisted layer–by–layer assembly to achieve simultaneously excellent self–extinguishing ability, antistatic property and antimicrobial activity. Especially, a novel hot–dog structured protective coating was designed through introducing polyaniline nanofibers into graphene nanosheets, which can exhibit unique structural advantages and give full play to the compound synergetic effect. More clearly, 3–aminopropyl triethoxysilane, ammonium polyphosphate and polyaniline were selected for phosphorus–silicon–nitrogen synergism in the assembled layer, while PANI nanofibers doped with various organic acids were penetrated into the graphene nanosheets for constructing more stable and efficient protective space. The optimized coated fabric exhibited the excellent self–extinguishing ability for 5 composite layers including phytic acid doped nanofiber, and a significantly enhanced LOI to 35.1 % from 18.1 % for neat cotton fabrics. Moreover, the peak heat release rate and the total heat release values were significantly declined by 78.3 % and 49.0 %, respectively. Furthermore, a low sheet resistance of 264.7 kΩ/sq for antistatic property, as well as remarkable growth inhibition of *E. coli* and *S. aureus* can be achieved. In addition, the fabrics also displayed the good washing durability. Therefore, such eco–friendly and facile large–scale fabrication approach has great potentials in application for multifunctional advanced textiles and could be employed to various other cellulose fibers.

1. Introduction

The cotton fabrics (CFs) have been extensively used as one of the most suitable fabrics both in clothing and industrial textiles owing to their comfortableness, hydrophilicity, high mechanical property, strong biocompatibility and biodegradability (Malucelli 2020; Qiu et al. 2018; Alongi and Malucelli 2015). However, the CFs suffer from their highly flammable nature with the limiting oxygen index value of about 18 %, and due to its porous and hydrophilic structure, are easy to encourage the growth of bacteria especially those thriving bacteria that can cause diseases in humans and induce the degradation of cellulose. To meet safety regulations and expand the use of cotton in textile applications, a significant number of surface treatment approaches have been developed for improving the protection performance by enhancing the flame retardant and antimicrobial properties of the CFs (Li et al. 2019a, 2020; Liu et al. 2020; Pan et al. 2015; Xue et al. 2020). Along with a remarkable improvement in quality of life and ever–growing consumer demands, there have been dramatic increases in the developing of functional fabrics, especially as protective functional textiles (e.g., electromagnetic interference shielding (Cheng et al. 2020; Wang et al. 2019; Zhang et al. 2019), antistatic (An et al. 2020), and UV–protection (Hu et al. 2015) and healthcare textiles (e.g., antimicrobial activity (Fang et al. 2015; Safi et al. 2020) and far–infrared emission (Hu et al. 2015). Many complex applications require multifunctional fabrics, generally by integrating the flame retardant, antistatic and antibacterial properties (An et al. 2020; Chang et al. 2014; Dong et al. 2015; Fang et al. 2016a; Lazar et al. 2020; Maráková et al. 2017; Zhang et al. 2020). Particular attention is devoted to meet additional strategic requirements from the industry and academia as next–generation wearable materials for a large variety of applications such as superhydrophobic (Guo et al.

2020; Wang et al. 2020a; Xue et al. 2020), electronic textile (Chen et al. 2016; Jedrzejczyk et al. 2019; Ramos et al. 2019; Zhao et al. 2020) and smart textile (Lima et al. 2018; Ren et al. 2017; Xie et al. 2020).

Although the field of surface treatment of the CFs has made great progress, to date, it is still a technical challenge to fabricate durable multifunction and maintain simultaneously their pristine performances. Generally multi–step chemical treatments of the CFs are carried out to obtain the multifunction, which might entail the high cost and complicated operations. Among all the surface treatment methods, LBL assembly approach has attracted widespread attention (Chen et al. 2016; Fan et al. 2018; Rawtani et al. 2014). Because it can easily fabricate high performance and versatility multilayer coating on the CF by adjustably selecting different functional cationic and anionic polyelectrolytes as assembly materials to control the final performance of cotton matrix (Qiu et al. 2018; Zhang et al. 2019). More importantly, most flame retardant coating can be precisely controlled and deposited at the surface of the protected textiles, so that it can achieve the highest protection under the very limited thickness and without affecting the bulk characteristics of cotton substrates (An et al. 2020; Lazar et al. 2020; Li et al. 2020; Malucelli 2020; Safi et al. 2020). Furthermore, multifarious potential functions have been exploited by alternating deposition of different functional cationic and anionic polyelectrolyte layers at room temperature and atmospheric pressure, using diluted and usually waterborne suspensions/solutions, thus limiting the environmental impact of the LBL treatments (Fang et al. 2016b; Malucelli 2020; Pan et al. 2015; Qiu et al. 2018; Zhao et al. 2015). Although it has many advantages, the multiple cycles of immersion and rinse processes also make it difficult in industrial applications. Fortunately, spray–assisted LBL can impart better performance due to its shorter processing time, lower weight gain and no risk of solution cross–contamination (Lazar et al. 2020; Zhao et al. 2015), making it more promising for industrial applications (Chang et al. 2014; Fan et al. 2018; Nooralian et al. 2016; Wang et al. 2020b). Furthermore, it is also highly desirable to generate nano– to micrometer size particles and prevent the aggregation of nanoparticles in a very short time frame (Fang et al. 2016b; Wang et al. 2018).

Commonly, thicker intumescent coating, higher flame retardant efficiency, but accompanying with the loss of the outstanding properties of the cotton such as softness, comfortableness, and mechanical properties. The construction of nanoscale coatings can effectively avoid the above problems because it can exert the molecular interaction between different layers and the synergistic effect of different elements (Lazar et al. 2020; Qiu et al. 2018). Moreover, it is very important to develop new intumescent coating with high flame retardant efficiency. With the increasing awareness of environmental protection, more and more biomass material and green intumescent were introduced into flame retardant coating as acid source, char–forming agent and blowing agent (Alongi and Malucelli 2015; Fang et al. 2016a). Nowadays, many new compounds have been developed intensively to improve the fire resistance of the CFs through the synergistic effect of phosphorus, nitrogen, and silicon (Li et al. 2019b; Liu et al. 2019). Zeng et al. 2020) prepared a phosphorus–nitrogen–silicon–based assembled multilayer coating, the coated fabric with a coatings content of 21.2 % obtained excellent flame retardancy with LOI value of 29.8 %.

Apart from the design of new highly efficient flame retardants, unique structures constructed by inorganic nanoparticles in the coating are playing an extraordinary role on the enhancement of the functions of the CFs (Qiu et al. 2018; Saadat et al. 2020; Tharmavaram et al. 2018). These inorganic nanoparticles mainly include nanoscale metal and metal oxides particles as well as two–dimensional materials such as graphene oxide (GO) (Li et al. 2019c; Sang et al. 2016; Zhao et al. 2020). It has been demonstrated that the GO have the potential to fulfill most requirements for use in conductive, antimicrobial and flame retardant coating thanks to their high carrier mobility, rich functional group, environmental stability and potential for low–cost production (Zhao et al. 2020). Especially, the brick wall structure of graphene is capable of protecting the substrate during combustion because of its high thermal stability and strong barrier effect accompanying with excellent antistatic and antimicrobial properties (Fang et al. 2015; Zeng et al. 2020). However, the number of processing steps was still high, mainly because the graphene was liable to stacking and often exhibit poor dispersion that is unbeneficial to flame–retardant effect. Note that the aggregation of the graphene sheets can be effectively suppressed by introducing the polyaniline (PANI) nanofibers as the stabilizer (He et al. 2012), and further construct confined space for the flame retardant. It is worth to point out that the PANI have also been exploited as highly efficient intumescent flame–retardant coatings, benefiting from the formation of graphitic structures during the burning that can enhance the thermal stability of the substrate (Bhattacharjee et al. 2019; Chang et al. 2020; Mao et al. 2013; Yuan et al. 2016; Zarrintaj et al. 2019). In addition, it is found that both the conductivity and the flame retardancy of the fabrics had a close relationship with the incorporation of doping acid (Chang et al. 2020; Mao et al. 2013; Wu et al. 2013).

In this work, quaternary compounds consisted of the GO, ammonium polyphosphate (APP), and PANI nanofibers doped with organic acid as an anionic polyelectrolytes, and 3–aminopropyl triethoxysilane (APTES) as a cationic specie would be used to fabricate the protective coating for the CFs by spray–assisted LBL assembly. Especially, one kind of unique hot–dog structure would be constructed by inserting PANI nanofibers into graphene nanosheets. It is believed that excellent self–extinguishment of the treated fabrics could be achieved, resulting from the strong combination of blowing agent, acid and carbon sources and unique structural advantage in the protective coating. Meanwhile, the GO and PANI in the coating could also ensure the CF with excellent antistatic and antibacterial properties. Comprehensive tests would be carried out to explore the structure and morphology, combustion behavior, thermal and electrical conductivity, anti–static behavior and so on. The nature of organic acids as the doping agents for PANI nanofibers on the flame retardant efficiency of the protective coating would be discussed. Besides, the durability under continuous washing was also investigated. The aim in this work would be focused on developing a facile, scalable, and effective approach to prepare such multifunctional CFs that could possesses simultaneously among self–extinguishment, conductivity and antimicrobial activity, and expand the application of the CFs in living and industrial fields.

2. Experimental

2.1 Materials

The CF with the density of 95 g/m^2 was supplied from Shandong Lichang Textile Science and Technology Co., Ltd. Natural flake graphite was purchased from Qingdao BCSM Co., Ltd. Ammonium polyphosphate (DP < 20), sarcosine and tannic acid were received from Shanghai Macklin Biochemical Co., Ltd. Other chemicals including APTES, aniline (≥ 99.5%), ammonium persulfate (APS), $FeCl_3$, carbon tetrachloride (CCl_4), phytic acid, sodium nitrate, potassium permanganate, hydrogen peroxide (30 %), H_2SO_4 (95–98 %), HCl (36.5–38 %) were purchased from Sinopharm Chemical Reagent Co., Ltd. (China). All of these chemicals were of laboratory grade and used as received. All solutions or suspensions were prepared with 18.2 MΩ deionized water.

2.2 Preparation of electrolyte solution

The microscale GO nanosheets with a thickness of approximately 1.8 nm were prepared according to our previous reports (Liang et al. 2015). The PANI nanofibers doped by HCl (named as PANI–H) were firstly obtained through interfacial polymerization at the water/ CCl_4 interface by using APS as an oxidant (Zeng et al. 2015), and then de–doped in 0.1 M ammonia solution. Subsequently, the nanofibers were re–doped in the aqueous solutions of organic acids including phytic acid, sarcosine and tannic acid, and noted as PANI–P, PANI–S and PANI–T, respectively. Their infrared spectra and thermogravimetric curves were provide in **Fig. S1** in Supplementary Materials. The anionic electrolyte was prepared by adding 500 mL deionized water to a mixture of GO (1 mg/mL), APP (5 wt. %) and PANI nanofibers (1mg/mL) under mechanical stirring to form a uniform aqueous dispersion. The cationic electrolyte was obtained by diluting 25.0 g APTES in 500 mL H_2SO_4 aqueous solution (5 wt. %, pH = 4) under stirring for 30 min.

2.3 Fabrication of multifunctional CFs

The CFs (500 mm · 200 mm) were horizontally fixed on the brandreth, and coated firstly by spraying GO solution. Then the quaternary compounds including APTES as a cationic polyelectrolytes and GO/APP/PANI nanofibers as an anionic specie were alternately sprayed to construct the multiple protection coating both sides of the fabrics as illustrated in Fig. 1. More specifically, the spray nozzle was 2.0 mm in inner diameter, and the spray gun was kept at a working distance of 50 cm from the fabric surface. The coated fabrics were dried at 70°C for 5 min after each spray. After 5 cycles, the coated fabrics were rinsed with deionized water and dried naturally. The coated fabric was noted as $(P–PANI)_5$ when the PANI nanofibers doped with phytic acid were intercalated into the GO layers as displayed in Fig. 1. It is necessary to point out that the number of bilayers deposited on the CF was optimized to ensure self–extinguish of the fabric.

2.4 Characterization

Surface morphologies of neat CF and treated fabrics as well as their char residues after vertical flame test were observed on a Hitachi SU–8010 field–emission scanning electron microscopy (FE–SEM).

The chemical structures were characterized on a Nicolet 8700 attenuated total reflection Fourier transform infrared (ATR–FTIR) spectrometer using 32 scans in the frequency region of 4000–400 cm^{-1}

at a 4 cm^{-1} resolution.

The graphitization degree of char residue was evaluated on a Renishaw inVia–Reflex Raman spectrometer with a He–Ne 632.8 nm laser.

Element analyses for neat CF and treated fabrics were carried out on an X–ray photoelectron spectrometer (XPS, Thermo Scientific ESCALAB 250Xi, USA) with Al Kα radiation (λ = 8.34 Å) as the excitation source.

The limiting oxygen index (LOI) values of neat CF and coated fabrics (150 mm × 58 mm) were measured by an oxygen index meter (JF–3, Jiangning, China) according to GB/T 5454–1997 standard.

Vertical flame tests (VFT) were performed accordance to GB/T 5455–2014 using a vertical burning instrument (CZF–3, Jiangning, China). The fabric (150 mm · 76 mm) was placed above butane burner and exposed to the flame for 5 s. The flame length of the burner was 40 ± 2 mm. The test was repeated 3 times for each sample, and the whole burning process was recorded by a digital video recorder.

Combustibility of evolved gases were evaluated on a microscale combustion calorimeter (Govmark, MCC–2). Typical test employed 5 ± 0.5 mg samples that undergone pyrolysis in a nitrogen stream flowing at 80 mL/min at a heating rate 20°C/min. The pyrolysis products of cotton were mixed with a 20 mL/min stream of oxygen prior to entering a 900 ^{o}C combustion furnace. All the tests were repeated 3 times for calculating the average % standard deviation.

The thermal stabilities were examined on a NETZSCH TG 209F1 thermogravimetric analyzer (TGA) from 30 to 700°C at a heating rate of 20°C/min under a nitrogen and air flow of 50 mL/min, respectively.

The thermal degradation processes were monitored on a NETZSCH TG 209F1 analyzer coupled with Nicolet 8700 FTIR spectrometer from 30 to 600°C at a heating rate of 20°C/min under a dynamic nitrogen flow of 50 mL/min.

The average surface resistances of the coated fabrics (5 cm · 5 cm) were obtained by 5 repeated measurements through four–point probe technique (RTS–8, Probes Tech, China) according to AATCC 76–2005.

The mechanical properties were measured with a universal testing machine (Instron 1185) according to the modified GB/T 3923.1–1997. The 250 × 30 mm^2 specimens were tested with a speed of 5 mm/min at room temperature.

The antimicrobial activities were qualitatively assessed against E. coli and S. aureus by the Kirby–Bauer test described by previously report (Fang et al. 2015). The MHB bouillon culture–medium (5×10^5 CFU/mL) was provided by Hope Bio–Technology Co., Ltd. All the fabrics with the size of 1 cm · 1 cm and medium were sterilized under a pressure of 0.1MPa and a temperature of 120^{o}C for 20min, and then immediately transferred to the drying oven and dried at 60^{o}C. *E. coli* and *S. aureus* were added into the

sterilized medium and kept in the constant temperature shaker at 37°C for overnight culture. The clean and diluted bacterial suspensions were exposed to visible light (Hitachi U–2900) and the optical density (OD) value after absorption was obtained.

Washing tests including standard washing and rinsing steps were performed according to GB/T 17595–1998. The fabric was washed at 40°C by using ECE non–phosphate reference detergent with the weight ratio of detergent to fabric of 20.

3. Results And Discussion

3.1 Surface morphology and composition

The coating process of quaternary composites on the surface of the CFs have been monitored by SEM observation and infrared characterization. As shown in Fig. 2**(a)**, neat CFs had relatively smooth surfaces. The CF has numerous active hydroxyl groups in its chemical structure, which would ensure the adhesion and distribution of coating materials on the surface. Thus the fabrics coated with the GO sheets and further by spraying APTES solution still exhibited very smooth surface. However, the slight increase in the surface roughness of the fabrics could be seen after GO/APP/PANI solution was sprayed into the surface of the CFs, and became rougher and rougher with further increase of the number of assembled layers accompanying with the fully coverage of the gaps among the cotton fibers by the GO sheets as shown in Fig. 2**(a)**. No obvious aggregation of the GO sheets and PANI nanofibers could be observed, and the good dispersion of GO sheets and PANI nanofibers could result in a noticeable barrier effect on mass and heat transfer as well as marked flame retardancy.

Furthermore, Fig. 2**(a)** also gives the SEM image of cross section for $(P–PANI)_5$, and apparently, the existence of nanoscale coating on the CF. By the way, the assembled content in the coated fabric was 15.3 wt. % for $(P–PANI)_5$. It is believed that the construction of nanoscale protective coatings could better exert the molecular interaction between different layers and the synergistic effect of different elements. Moreover, the PANI nanofibers were intercalated into the GO layers enlarge the gaps between the GO sheets, being similar to the hot–dog structure as displayed in the insert in Fig. 2**(a)**, which could form nearly closed subspace to resist heat and oxygen. By the way, the average diameter of PANI nanofibers from SEM images was about 79.6 ± 10.3 nm of PANI–P as illustrated in Fig. 2**(a)**. These results indicated that the easy–operating LBL spraying assembly could form a homogeneous and ultrathin coating on the surface of the CFs (Wang et al. 2020b).

The chemical structures of the CFs before and after coating were characterized by ATR–FTIR spectroscopy as displayed in Fig. 2**(b)**. The main characteristic peaks for neat CF could be seen such as the broad absorption peak at 3260–3500 cm^{-1} could be assigned to stretching vibrations of O–H groups, at 2903 cm^{-1} to CH_2 groups, around 1429, 1366 and 1318 cm^{-1} to C–H in–plane bending, deformation stretching and wagging, respectively, and about 1155 and 1024 cm^{-1} to C–O–C stretching vibrations of the cellulose backbone (Fang et al. 2016a, 2016b; Pan et al. 2015; Zeng et al. 2020). When the CF was coated with GO, two new peaks located at 1202 and 1051 cm^{-1} could be corresponded to the C–O (epoxy

and alkoxy) stretching in GO, respectively (Wang et al. 2019). After further spraying APTES solution, a new peak at 1521 cm^{-1} appeared, which was associated to $-NH_3^+$ groups of hydrolyzed APTES (Wang et al. 2018). Furthermore, after coating with the GO sheets intercalated with PANI nanofibers, two main characteristic peaks could be observed at about 1590 and 1453 cm^{-1}, which could be attributed to quinonoid and benzenoid ring–stretching vibrations of the PANI, respectively (Liang et al. 2015; Zeng et al. 2015). The peak at approximately 3053 cm^{-1} could be ascribed to the $-NH_4-$ vibration bands in APP molecules (Fang et al. 2015; Zhao et al. 2015). Moreover, Strong interaction between the carboxylate groups of GO and $-NH_3^+$ groups of hydrolyzed APTES or PANI occurred, resulting in the appearance of three new peaks at near 1618, 1436, and 1312 cm^{-1} corresponding to amide I, II, and III, respectively (Wang et al. 2018). More clearly, apart from those for cellulose, the thicker assembled layer, the stronger infrared absorptions for the coating composition, indicating that the multifunctional coating containing APTES hydrolysis and GO/APP/PANI were successfully deposited on the surface of the CFs through spray assisted LBL assembly. These results could be further supported by observing the existence of nitrogen, silicon and phosphorus contents for the coated fabrics with PANI nanofibers doped by various organic acids in XPS spectra as shown in Fig. 2**(c)**. In contrast, only carbon and oxygen contents appeared for neat CF. The chemical components of the CFs before and after coating was listed in **Table S1**. The highest phosphorus content could be achieved by introducing phytic acid doped PANI nanofibers. During the burning process, phosphorus–containing compounds could promote dehydration and carbonization. More importantly, excellent self–extinguishing characteristics could be expected by bringing into full play the compound synergetic effect and unique advantage of hot–dog structure in the protective coating.

3.2 Flame retardancy

To evaluate the flammability of the CFs, vertical burning test and LOI measurement were used to visually show the actual ignition and diffusion behavior. Figure 3**(a)** presents surface morphologies of char residues for neat CF and coated fabrics after vertical burning test, and the insert gives the real–time images of the char residues. The LOI values for neat CF and coated fabrics as well as their flammability data were listed in **Table S2**. After ignition, the CF burned vigorously and spread upward rapidly, and 17 s afterglow could be obviously seen after the flame was extinguished, showing poor fire safety. In contrast, after being coated by APTES and GO/APP/PANI for 5 bilayers, all coated fabrics were hard to ignite, where the flame extinguished immediately once removing the fire source, and the char length were 6.8 cm, 5.8 cm, 6.4 cm and 8.1 cm for $(H–PANI)_5$, $(P–PANI)_5$, $(S–PANI)_5$ and $(T–PANI)_5$, respectively. The LOI value was 18.1 %, 31.6 %, 35.1 %, 33.7 %, and 30.2 % for neat CF, $(H–PANI)_5$, $(P–PANI)_5$, $(S–PANI)_5$, and $(T–PANI)_5$, respectively, indicating great improvement on flame retardant performance of the CF by the protective coating. Among all the coated fabrics, the $(P–PANI)_5$ had the largest LOI value, which could be benefiting from the highest phosphorous content when phytic acid was used as the dopant for PANI nanofibers. Furthermore, it can be observed in low–magnification SEM images as illustrated in Fig. 3**(a)** that all the fabrics could maintain original textile structure of the CFs after combustion except neat CF, which could contributed to the flame retardant effect of the assembly layer. It is necessary to point out

that almost all the uncoated fabric was burned out, and very less residue could be left. Benefiting from phosphorus–nitrogen–silicon synergetic effect, the coating could protect the CFs from fire to some extent, and the char layer formed during combustion could serve as stable thermal insulating layer and shielded the internal cellulose from outside heat and oxygen, as a result, the further thermal decomposition and combustion of the cotton would be efficiently suppressed. It is well known that the high flame retardant efficiency of the intumescent coating was attributed to the strong combination of blowing agent, acid and carbon sources. As shown in Fig. 3**(a)**, many number of bubbles could be seen in high–magnification SEM images for the coated fabrics especially for $(P–PANI)_5$ and $(S–PANI)_5$ due to the expansion of char and the release of voltaic compounds produced during combustion (Pan et al. 2015; Xie et al. 2020). These intumescent bubbles that were related to the nitrogen content in the coating. No surprisingly, $(P–PANI)_5$ and $(S–PANI)_5$ had relatively high nitrogen content as listed in **Table S1**. In addition, less gaps among all the fibers could be found in their char layers especially for $(P–PANI)_5$ as displayed in Fig. 3**(a)**, in which APP and phytic acid doped PANI could act as both blowing agent and acid source. The compact residual char layer could stop the flame spread effectively, thus the $(P–PANI)_5$ possessed excellent self–extinguishing ability.

Most of widely used flame retardants are designed to inhibit the thermal degradation of the CF through promoting the formation of a thermally stable char. The swollen carbon layer formed by the assembled layer could act as a physical barrier to insulate the release of flammable pyrolysis products to combustion and the transfer of oxygen into the condensed phase, thus preventing the fabrics from further burning (Liu et al. 2019; Li et al. 2019c; Mao et al. 2013). Therefore the char residues of the CFs after vertical flame test were further characterized by Raman spectroscopy. As displayed in the Fig. 3**(b)**, all the char layers derived from neat CF and coated fabrics exhibited two characteristic bands for graphitic structure, in which the G–band (1588 cm^{-1}) was ascribed to the stretching vibration of sp^2–bonds carbon atoms in the aromatic layers of the crystalline graphite, while the D–band (1360 cm^{-1}) to the vibration of carbon atoms with dangling bonds for the amorphous carbons (Wang et al. 2018). Generally, the area ratio of the D and G bans (A_D/A_G) is used to estimate the graphitization degree of char residue, where A_D and A_G are the integrated area of the D and G bands by Lorentz fitting, respectively (Zeng et al. 2020). Compared with neat CF, all the coated fabrics had much lower A_D/A_G ratio, and further the $(P–PANI)_5$ possessed the lowest A_D/A_G ratio of 2.38 among all the fabrics. Obviously, the thicker assembled layer on the CF, the larger graphitization degree and higher thermally stability of char layer. Meanwhile, the nature of organic acids also played an important role in the flame retardant properties of the CFs. Apparently, the introducing of phytic acid could provide more effective physical barrier for preventing the diffusion of flammable volatilized products as well as the oxygen and heat entering the condensed phase.

The combustibility and fire hazard of neat CF and coated fabrics were finally evaluated by MCC test as presented in Fig. 4. During the test, the cotton was pyrolyzed in nitrogen, and the volatiles produced were further burned in the presence of oxygen. The data about total heat release (THR), temperature at peak heat release (T_p) and peak heat release rate (pHRR) were summarized in **Table S2**. As shown in HRR

curves, compared with neat CF, all the coated fabric were pyrolyzed earlier, and the T_p decreased by about 60–75 ^{o}C. This phenomenon was attributed to the catalytic action of phosphorus–containing assembled layers that could promotes the cotton to dehydrate at lower temperature (Fang et al. 2015). Moreover, the coated fabrics also had lower pHRR and THR values, which could result from strong char forming effect. In other words, spray assisted LBL assembly could reduce the production of combustible gas and enhance the flame retardancy of the CFs (Fang et al. 2015, 2016a; Zhang et al. 2019). More clearly, the value of pHRR decreased by 78.3 % from 277.5 W/g at 390.8°C for cotton fabric to 60.2 W/g at 314.7°C for $(P–PANI)_5$, while the THR value reduced by 49.0 % from 14.3 kJ/g to 7.3 kJ/g. The existence of the flame retardant layer greatly reduced the risk of fires to spread to unburned parts of the coated fabric and also made it easier to extinguish (Fang et al. 2015).

3.3 Thermal stability

The thermal degradation behaviors under both air and nitrogen atmospheres of neat CF and coated fabrics were analyzed by TGA and DTG as depicted in Fig. 5. The initial degradation temperature ($T_{-5\%}$), the maximum mass loss temperature (T_{max}) and char residue percentage at 700 ^{o}C were obtained from TGA curves and found in Table 1. As revealed in Fig. 5, all the fabrics mainly exhibited three degradation steps under air atmosphere (Fang et al. 2015; Zeng et al. 2020; Zhou et al. 2020). The first step (70–120 ^{o}C) could be ascribed to the removal of the absorbed water, the second step (230–400 ^{o}C) to the dehydration and decarboxylation reactions of cellulose, and the last step (450–550 ^{o}C) to the further decomposition of residual char that could generate volatile gases CO_2 and CO. All the coated fabrics especially the $(P–PANI)_5$ had much lower value of $T_{-5\%}$ and T_{max} compared with neat CF, indicating that the decomposition process was carried out in advance through promoting dehydration and carbonization induced by phosphoric acid derivatives from APP and phytic acid, favoring the residue formed and enhancing the thermal stability (Zeng et al. 2020; Zhou et al. 2020). Meanwhile, the more char residue was produced, the less flammable volatiles would be generated, being in favor of the enhancement on the flame retardancy of the CFs. The increased char residue could act as a thermal insulating barrier to inhibit mass/heat transfer between the CF and surroundings, and thus suppress the further decomposition of the cotton in higher temperature. The content of residual char at 700 ^{o}C increased significantly from 1.0 wt. % for neat CF to 11.4, 16.7, 12.6 and 10.3 wt. % for $(H–PANI)_5$, $(P–PANI)_5$, $(S–PANI)_5$, and $(T–PANI)_5$, respectively. Apparently, the $(P–PANI)_5$ exhibited the highest thermal stability under nitrogen atmosphere as listed in Table 1. These results indicated that the APTES–GO/APP/PANI assembled layer could improve greatly the flame retardancy of the CF by promoting the formation of thermally stable char layer, and the highest thermal stability could be achieved when phytic acid was applied as the doped acid.

Unlike in air, the representative TGA and DTG curves under nitrogen atmosphere exhibited very different features, and all the fabrics were composed of two main degradation steps appeared in TGA curves under nitrogen atmosphere. As displayed in Fig. 5, compared with neat cotton, all the coated fabrics had similar lower value of $T_{-5\%}$ (above 25 ^{o}C) and earlier degradation step (above 39 ^{o}C), being mainly attributed to the potentiation of the cotton by phosphor–containing retardant coating (Pan et al. 2015;

Zhang et al. 2019). Furthermore, all the coated fabrics revealed much higher thermal stabilities at temperature ranging from 350–700 ^{o}C, illustrating the formation of the protective char layer produced from the intumescent coating at high temperature (Chang et al. 2014; Wang et al. 2020a). Particularly, the content of residual char for the $(P–PANI)_5$ increased by about 347.7 % compared with that for neat CF. Note that the char yields at 700 ^{o}C for all the coated fabrics under nitrogen atmosphere were notably higher than those under air as illustrated from Table 1. It is concluded that the thermal stability of the coated fabrics could be improved because the oxidation degradation of the char layer could be effectively inhibited under nitrogen atmosphere (Alongi and Malucelli 2015). Thus, the APTES–GO/APP/PANI assembled layer could improve the char yields, hinder the formation rate of volatile compounds and diffusion of volatile gases to the flame zone, as a result, the significant improvement of flame retardancy of the CF could be achieved.

Table 1
Parameters obtained from TGA curves for neat CF and coated fabrics under air and nitrogen atmospheres.

Fabrics	Weight gain (wt. %)	$T_{-5\%}$ (℃)		T_{max} (℃)		Char residue at 700 ℃ (wt. %)	
		Air	N_2	Air	N_2	Air	N_2
CF	0	265.5	264.5	361.6	379.9	1.0	8.6
$(H–PANI)_5$	14.1	241.8	233.2	320.7	330.0	11.4	33.7
$(P–PANI)_5$	15.3	187.0	212.4	304.5	322.2	16.7	38.5
$(S–PANI)_5$	15.7	239.4	222.9	321.2	338.2	12.6	34.1
$(T–PANI)_5$	14.8	194.2	239.1	320.1	340.5	10.3	32.7

The gas ingredients during the thermal degradation process of neat CF and $(P–PANI)_5$ were detected with thermogravimetric analysis–infrared spectrometry (TG–IR) test. Figure 6 shows the 3D images of the gaseous compounds during thermal degradation process. Obvious difference on infrared absorption for thermal degradation products could be directly observed. Compared with neat CF, the coated fabric could release gaseous compounds at relatively low temperature. For neat CF, the main evolved gasses contained hydrocarbon compounds (2817 cm^{-1}), carbonyl compounds (1745 cm^{-1}), CO_2 (2354 cm^{-1}), CO (2177 cm^{-1}) and methanol (1089 cm^{-1}). In contrast, there are almost no absorption peaks for hydrocarbon compounds and methanol appeared in the pyrolysis products of the $(P–PANI)_5$, and less H_2O and CO_2 as well as inflammable gases than those released by neat CFs. The improvement on the flame retardant properties of the cotton could be attributed to thermal decomposition of flame retardant assembled layers that could react with the CFs to alter its thermal decomposition process. Moreover, after

normalized with the total mass of the fabric, Fig. 6 further presents the total absorption peak intensity and several main absorption bands of the volatilized products for neat CF and $(P–PANI)_5$ including H_2O (3565 cm^{-1}), CO_2 (2354 cm^{-1}), CO (2177 cm^{-1}) and carbonyl compounds (1745 cm^{-1}) (Pan et al. 2020; Zeng et al. 2020; Zhang et al. 2019). From the total absorption curves, the total gas release peak of the CF appeared at 1061 s, while 922 s for the $(P–PANI)_5$, indicating that the existence of APTES–GO/APP/PANI protective layer could accelerate the thermal degradation of the CF, which was consistent with the result obtained from TGA curve. However, it can be clearly seen from the absorption curve of CO that the absorption peak of CO had an obvious hysteresis compared to neat CF, indicating that the introducing of PANI nanofibers doped with phytic acid could delay the release of flammable CO gas. According to the Lambert–Beer law, a linear relationship between the gas concentration and absorption intensity at a specific wavenumber would be obeyed. As illustrated in Fig. 6, all the intensities of pyrolysis products for $(P–PANI)_5$ were much lower than those of neat CF. Furthermore, CO and CO_2 are the two toxic gases that mainly threaten the life and health of escapees. Therefore, it is concluded that the coated fabric could obviously reduce the release of toxic gas during the thermal degradation process. These results further indicated that the assembled layers on the surface of the CFs could provide a beneficial physical barrier that would restrain the transfer of mass and heat and insulate oxygen, resulting in the reduction in THR and HRR obtained by MCC test.

3.4 Mechanical, antistatic and antimicrobial properties

Generally, the thicker flame retardant coating on the surface of the CFs, the better self–extinguishing performance, but the worse in the flexibility. Figure 7 **(a)** presents the stress–strain curves for the CFs before and after coating. The ensile strength was 64.3, 65.8, 65.2, 65.6 and 66.2 N, while elongation at break was 33.0 %, 34.0 %, 33.4 %, 33.5 % and 34.5 % for neat CF, $(H–PANI)_5$, $(P–PANI)_5$, $(S–PANI)_5$ and $(T–PANI)_5$, respectively. Clearly, slight improvement on the mechanical properties of the CF could be observed by introducing ultrathin protective coating as illustrated in Fig. 2**(a)**, implying the surface treatment through spray–assisted layer–by–layer assembly did not damage the structure of the cotton fibers.

To attest the influence of the coatings on the electrical properties of the CF, the sheet resistance (Rs) was measured for all the coated fabrics. The Rs of neat CF could not be detected due to the lack of conductivity. On the contrary, all the coated fabrics possessed excellent antistatic properties due to a conducting network constructed with GO sheets and PANI nanofibers on the surface of the CF as shown in Fig. 7**(b)**. Among all the coated fabrics, the $(P–PANI)_5$ had the lowest Rs of 264.7 kΩ/sq, which could be attributed to highly conductive pathways by introducing phytic acid doped PANI nanofibers with relative high conductivity (Zhou et al. 2020).

The GO sheets were intercalated with PANI nanofibers to form the protective layer that not only enhanced mechanical properties but also improved antibacterial activity against the bacteria of the coated fabrics compared with neat CF. In fact, it has been demonstrated that the CF coated with PANI alone also showed antibacterial activity to some extent (Maráková et al. 2017). As displayed in Fig. 7**(c)**, two typical bacteria,

Gram negative *Escherichia coli* (*E. coli*) and Gram positive *Staphylococcus aureus* (*S. aureus*), were used to compare the antibacterial properties of neat CFs and coated fabrics. The responses to visible light (wavelength of 600 nm) of the CF were almost the same for both *E. coli* and *S. aureus*, and the value was about 1.15. For *E. coli* cultivated in the presence of $(H–PANI)_5$, the response value decreased to about 0.62, but only 0.31 for $(P–PANI)_5$. More clearly, the antibacterial property was greatly enhanced, which could be attributed to the combined effect of both the GO and PANI coated on the surface of the CF. It is believed that the GO could directly contact with bacteria and lead to incidence of irreversible damages and finally destruct the structures of bacterial cell, while PANI nanofibers could kill bacteria by exerting cation adsorption (Fang et al. 2015). Furthermore, the antibacterial performance of the coated fabric improved significantly when the HCl was replaced by to phytic acid. However, for *S. aureus* cultivated in the presence of all the coated fabrics, no signal could be detected and the bacteria did not breed any more as illustrated in Fig. 7**(c)**. Apparently, the coated fabric was more effective against the Gram negative *S. aureus* compared than the Gram positive *E. coli*. In addition, the Kirby–Bauer test was used to determine the antimicrobial actions of coated fabrics on *E. coli* and *S. aureus*. It was found that the $(P–PANI)_5$ formed a zone of inhibition compared to neat CF as shown in Fig. 7**(c)**, which further demonstrated that the coated fabric could inhibit the growth of bacteria.

3.5 Comparison and washing durability

The flame retardant, antistatic and antimicrobial performances for the $(P–PANI)_5$ were compared with various multifunctional materials reported previously as presented in Table 2. The excellent self–extinguishing ability, antistatic property and antimicrobial activity were simultaneously achieved, which could contributed to the synergetic effects among nitrogen–, silicon– and phosphorus–based compounds in the protective coating accompanying with the unique structural advantage of the hot–dog that could ensure the good dispersion of the GO, and provide nearly closed subspace to and resist heat and oxygen. Generally, the more coating load, the stronger functional effect of the coated fabric. However, as the coating load content increases, the flexibility of the fabric will become worse. In our work, the loading mass for the $(P–PANI)_5$ was 15.3 wt. %, and the construction of nanoscale protective layer as shown in Fig. 2**(a)** could enhance the molecular interaction between different layers, and take full advantage of the synergistic effect of different elements. Besides, this kind of multifunctional cotton fabric were fabricated by low–cost and environmentally–friendly spray–assisted layer–by–layer assembly.

Table 2
Comparison of flame retardant, antistatic and antimicrobial performance for various multifunctional coatings

Weight gain / wt. %	LOI / %	VFT Level	Rs / (kΩ/sq)	Antimicrobial / %	Ref
1.3	19.5	V1		90	Fang et al. 2015
4.8		V1		100	Fang et al. 2016a
5.9		V1	100	99.8	Chen et al. 2016
8.0	27.0	V0		99.8	Li et al. 2020
15.3	35.1	V0	264.7	100	**This work**
16.0	30.5	V0		89	Safi et al. 2020
18.6	31.9	V0		97	Dong et al. 2015
23.9	33.9	V0	1260	100	Zeng et al. 2020
25.0	31.2	V0	1.07		Zhang et al. 2020
26.3	23.6	V1	49.7		An et al. 2020
31.7	37.0	V0	0.41		Zhang et al. 2019
40.6	36.5	V0	1.49		Cheng et al. 2020
41.0			7700	88	Ramos et al. 2019
49.2	28.6	V0	32.6		Chang et al. 2020
53.8	31.9	V0	749		Wu et al. 2013
54.1	34.9	V0	47.7		Mao et al. 2013

The influences of the nature of organic acids on the performances of the coated fabrics was also compared as displayed in Fig. 8. The mass loading of the protective coating was about 14.1, 15.3, 15.7, and 14.8 wt. % for $(H–PANI)_5$, $(P–PANI)_5$, $(S–PANI)_5$, and $(T–PANI)_5$, respectively. It is found that the mass loading at the same number of assembled layers increased when the HCl was replaced by organic acids. Furthermore, the $(T–PANI)_5$ exhibited the best antibacterial performance, but the lowest LOI value and the highest Rs. By contrast, the $(P–PANI)_5$ had not only the best flame retardancy but also had the lowest Rs, but its antibacterial property was inferior to that for $(T–PANI)_5$. In other words, the $(P–PANI)_5$ had the best comprehensive performance among all the coated fabrics. In addition, the washing durability of the coated fabric was evaluated according to GB/T 17595–1998. As illustrated in Fig. 8, the $(P–PANI)_5$ exhibited a decrease in the mass loading from 15.3 wt. % to 13.9 wt. %, an increase in the Rs from 264.7 to 338.6 kΩ/sq, and a reduce in the LOI value from 35.1 % to 29.5 % after 12 laundering cycles. Especially, the $(P–PANI)_5$ could still possessed highly efficient flame retardancy and antistatic

property after laundering treatments. The good washability could be attributed to the covalent bonding between adjacent layers as well as strong π–π conjugation and hydrogen bonding interaction in unique hot–dog structure. In addition, strong adhesion of the assembled layers on the surface of the CF could be obtained, which could attributed to numerous hydroxyl groups in the chemical structure of the cotton. Overall, spray–assisted layer–by–layer assembly presented in this work could provide a simple but very effective approach for the fabrication of washable multifunctional CFs and other cellulose substrates. By the way, the hot–dog structure could also be constructed by other one–dimensional nanomaterials such as surface modified carbon nanotubes and halloysite nanotubes (Pandey et al. 2017; Rawtani et al. 2017; Xue et al, 2020).

3.6 Possible functional mechanism

Finally, according to the conclusions above, the possible functional mechanism could be explained by the compound synergetic effect and unique structural advantage in the protective coating. Generally, the excellent self–extinguishment of the coated fabrics could be achieved through the synergistic effect of phosphorus, nitrogen, and silicon by using intumescent flame retardants as blowing agent, acid and carbon sources. When exposed to the fire, the protective coating favored the formation of intumescent char that served as a thermal insulating layer and shielded the internal cellulose from outside heat and oxygen. Furthermore, the construction of nanoscale protective coatings by spray assisted layer–by–layer assembly could better exert the molecular interaction between different layers, as a result, stronger synergistic effect of different elements could be achieved. Moreover, more phosphorus content achieved by introducing phytic acid doped PANI nanofibers could promote dehydration and carbonization, and especially relatively compact char layer could protect the underlying cotton fabrics from spreading the fire and stop further oxidative degradation of cotton fabrics. The excellent self–extinguishing ability of the coated fabrics also attributed to the inorganic nanosilica produced during the combustion, which could act as a barrier to heat, fuel, and oxygen transfer, as well as unique structure of the hot–dog formed by intercalating PANI nanofibers into the GO sheets, which could provide a nearly closed space to prevent the release of flammable pyrolysis products to combustion and the oxygen and heat entering the condensed phase (Fang et al. 2016b; Zeng et al. 2020). These results indicated that the APTES–GO/APP/PANI assembled layer could improve greatly the flame retardancy of the CF by promoting the formation of thermally stable char layer and hindering the formation rate of volatile compounds and diffusion of volatile gases to the flame zone (Zhou et al. 2017). Because the GO and PANI also have the potential to fulfill most requirements for use in conductive and antimicrobial activity (Chang et al. 2020), it is not surprising that the coated fabrics could exhibited sufficient antistatic and excellent antimicrobial properties.

4. Conclusion

Multifunctional cotton fabric that could possess simultaneously excellent self–extinguishing ability, antistatic property and antimicrobial activity was fabricated through spray assisted layer–by–layer assembly approach. More detailedly, the negatively charged solution consisting of graphene, PANI

nanofibers doped with different organic acids and APP, as well as positively charged solution of APTES were alternately deposited onto the surface of the CF, and especially unique hot–dog structure was designed by introducing PANI nanofibers into graphene nanosheets. The construction of nanoscale protective layer and unique hot–dog structure could bring into full play the compound synergetic effect and unique structural advantage in the protective coating. The best comprehensive performance can be obtained by using phytic acid doped PANI nanofibers among all the coated fabrics. More clearly, the $(P–PANI)_5$ had high LOI value of 35.1 % at the mass loading of 15. 3 wt. %. Moreover, the peak heat release rate and the total heat release values were greatly reduced by 78.3 % and 49.0 % compared with those for neat cotton, respectively. Furthermore, good antistatic and excellent antimicrobial activity against *E. coli* and *S. aureus*. In addition, the fabrics also exhibited the good washing durability. It is believed that such eco–friendly and facile large–scale fabrication approach could promote the great development of cheap hybrid nanocoating for multifunctional advanced textiles.

Declarations

Declaration of competing interest

The authors declare that they have no known competing financial interests or personal relationships that could have appeared to influence the work reported in this paper.

Acknowledgements

The authors gratefully acknowledge the financial support from National Natural Science Foundation of China (21875032). Dr. Zeng also thanks the financial support from the Fundamental Research Funds for the Central Universities (CUSF–DH–D–2017040).

References

1. Alongi J, Malucelli G (2015) Cotton flame retardancy: state of the art and future perspectives. RSC Adv 5(31):24239–24263
2. An W, Ma JZ, Xu QN, Fan QQ (2020) Flame retardant, antistatic cotton fabrics crafted by layer–by–layer assembly. Cellulose 27(14):8457–8469
3. Bhattacharjee S, Joshi R, Chughtai AA, Macintyre CR (2019) Graphene modified multifunctional personal protective clothing. Adv Mater Interfaces 6(21):1900622
4. Chang S, Slopek RP, Condon B, Grunlan JC (2014) Surface coating for flame–retardant behavior of cotton fabric using a continuous layer–by–layer process. Ind Eng Chem Res 53(10):3805–3812
5. Chang ZY, An XH, Qian XR (2020) High mass loading polyaniline layer anchored cellulose fibers: Enhanced interface junction for high conductivity and flame retardancy. Carbohydr Polym 230:115660

6. Chen X, Fang F, Zhang X, Ding X, Wang Y, Chen L, Tian X (2016) Flame–retardant, electrically conductive and antimicrobial multifunctional coating on cotton fabric via layer–by–layer assembly technique. RSC Adv 6(33):27669–27676
7. Cheng WH, Zhang Y, Tian WX, Liu JJ, Lu JY, Wang BB, Xing WY, Hu Y (2020) Highly efficient MXene–coated flame retardant cotton fabric for electromagnetic interference shielding. Ind Eng Chem Res 59(31):14025–14036
8. Dong C, Lu Z, Zhang F (2015) Preparation and properties of cotton fabrics treated with a novel guanidyl– and phosphorus–containing polysiloxane antimicrobial and flame retardant. Mater Lett 142:35–37
9. Fan Q, Ma J, Xu Q, An W, Qiu R (2018)) Multifunctional coatings crafted via layer–by–layer spraying method. Prog Org Coat 125:215–221
10. Fang F, Xiao DZ, Zhang X, Meng YD, Chen C, Bao C, Ding X, Cao H, Tian XY (2015) Construction of intumescent flame retardant and antimicrobial coating on cotton fabric via layer–by–layer assembly technology. Surf Coat Tech 276:726–734
11. Fang F, Chen X, Zhang X, Cheng C, Xiao D, Meng Y, Ding X, Zhang H, Tian X (2016a) Environmentally friendly assembly multilayer coating for flame retardant and antimicrobial cotton fabric. Prog Org Coat 90:258–266
12. Fang F, Tong B, Du T, Zhang X, Meng Y, Liu X, Tian X (2016b)) Unique nanobrick wall nanocoating for flame–retardant cotton fabric via layer–by–layer assembly technique. Cellulose 23(5):3341–3354
13. Guo W, Wang X, Huang J, Zhou Y, Cai W, Wang J, Song L, Hu Y (2020) Construction of durable flame–retardant and robust superhydrophobic coatings on cotton fabrics for water–oil separation application. Chem Eng J 398:125661
14. Hu X, Tian M, Qu L, Zhu S, Han G (2015) Multifunctional cotton fabrics with graphene/polyurethane coatings with far–infrared emission, electrical conductivity, and ultraviolet blocking properties. Carbon 95:625–633
15. He W, Zhang WN, Li Y, Jing XL (2012) A high concentration graphene dispersion stabilized by polyaniline nanofibers. Synthetic Met 162(13):1107–1113
16. Jedrzejczyk M, Makowski T, Svyntkivska M, Piorkowska E, Mizerska U, Fortuniak W, Brzezinski S, Kowalczyk D (2019) Conductive cotton fabric through thermal reduction of graphene oxide enhanced by commercial antioxidants used in the plastics industry. Cellulose 26(4):2191–2199
17. Lazar ST, Kolibaba TJ, Grunlan JC (2020) Flame–retardant surface treatments. Nat Rev Mater 5(4):259–275
18. Li P, Wang B, Xu YJ, Jiang Z, Dong C, Liu Y, Zhu P (2019a) Ecofriendly flame–retardant cotton fabrics: preparation, flame retardancy, thermal degradation properties, and mechanism. ACS Sustain Chem Eng 7(23):19246–19256
19. Li P, Wang B, Liu YY, Xu YJ, Jiang ZM, Dong CH, Zhang L, Liu Y, Zhu P (2020) Fully bio–based coating from chitosan and phytate for fire–safety and antibacterial cotton fabrics. Carbohydr Polym

237:116173

20. Li S, Lin X, Liu Y, Li R, Ren X, Huang TS (2019b) Phosphorus–nitrogen–silicon–based assembly multilayer coating for the preparation of flame retardant and antimicrobial cotton fabric. Cellulose 26(6):4213–4223
21. Li Y, Cao CF, Li SN, Huang HJ, Mao M, Zhang JW, Wang PH, Guo KY, Gong LX, Zhang GD, Zhao L, Guan LZ, Wan YJ,.Tang LC, Mai YW (2019c) In situ reactive self–assembly of a graphene oxide nano–coating in polymer foam materials with synergistic fire shielding properties. J Mater Chem A 7(47):27032–27040
22. Liang BL, Qin ZY, Li T, Dou ZJ, Zeng FX, Cai YM, Zhu MF, Zhou Z (2015) Poly (aniline–co–pyrrole) on the surface of reduced graphene oxide as high–performance electrode materials for supercapacitors. Electrochim Acta 177:335–342
23. Lima RM, Alcaraz–Espinoza J, Silva FA, Oliveira HP (2018) Multifunctional wearable electronic textiles using cotton fibers with polypyrrole and carbon nanotubes. ACS Appl Mater Interfaces 10(16):13783–13795
24. Liu J, Dong C, Zhang Z, Kong D, Sun H, Lu Z (2020) Multifunctional flame–retarded and hydrophobic cotton fabrics modified with a cyclic phosphorus/polysiloxane copolymer. Cellulose 27(6):3531–3549
25. Liu M, Huang S, Zhang G, Zhang F (2019) Synthesis of P–N–Si synergistic flame retardant based on a cyclodiphosphazane derivative for use on cotton fabric. Cellulose 26(12):7553–7567
26. Malucelli G (2020) Sol–gel and layer–by–layer coatings for flame–retardant cotton fabrics: recent advances. Coatings 10(4):333–351
27. Maráková N, Humpolíček P, Kašpárková V, Capakova Z, Martinkova L, Bober P, Trchova M, Stejskal J (2017) Antimicrobial activity and cytotoxicity of cotton fabric coated with conducting polymers, polyaniline or polypyrrole, and with deposited silver nanoparticles. Appl Surf Sci 396:169–176
28. Mao H, Wu XN, Qian XR, An XH (2013) Conductivity and flame retardancy of polyaniline–deposited functional cellulosic paper doped with organic sulfonic acids. Cellulose 21(1):697–704
29. Nooralian Z, Gashti M, Ebrahimi I (2016) Fabrication of a multifunctional graphene/polyvinylphosphonic acid/cotton nanocomposite via facile spray layer–by–layer assembly. RSC Adv 6(28):23288–23299
30. Pan HF, Wang W, Pan Y, Song L, Hu Y, Liew KM (2015) Formation of self–extinguishing flame retardant biobased coating on cotton fabrics via layer–by–layer assembly of chitin derivatives. Carbohydr Polym 115:516–524
31. Pandey G, Munguambe DM, Tharmavaram M, Rawtani D, Agrawal YK (2017) Halloysite nanotubes: An efficient 'nano–support' for the immobilization of α–amylase. Appl Clay Sci 136:184–191
32. Qiu XQ, Li ZW, Li XH, Zhang ZJ (2018) Flame retardant coatings prepared by layer by layer assembly: a review. Chem Eng J 334:108–122
33. Ramos AR, Tapia AK, Piñol CM, Lantican NB, Mundo ML, Manalo RD, Herrera MU (2019)) Morphological, electrical and antimicrobial properties of polyaniline–coated paper prepared via a

two–pot layer–by–layer technique. Mater Chem Phys 238:121972

34. Rawtani D, Agrawal Y (2014) Emerging strategies and applications of layer–by–layer self–assembly. Nanobiomedicine 1:8
35. Rawtani D, Pandey G, Tharmavaram M, Pathak P, Akkireddy S, Agrawal YK (2017) Development of a novel 'nanocarrier' system based on Halloysite Nanotubes to overcome the complexation of ciprofloxacin with iron: An in vitro approach. Appl Clay Sci 150:293–302
36. Ren JS, Wang CX, Zhang X, Carey T, Chen KL, Yin YJ, Torrisi F (2017) Environmentally–friendly conductive cotton fabric as flexible strain sensor based on hot press reduced graphene oxide. Carbon 111:622–630
37. Safi K, Kant K, Bramhecha I, Mathur P, Sheikh J (2020) Multifunctional modification of cotton using layer–by–layer finishing with chitosan, sodium lignin sulphonate and boric acid. Int J Biol Macromol 158:903–910
38. Saadat S, Pandey G, Tharmavaram M, Braganza V, Rawtani D (2020) Nano–interfacial decoration of Halloysite Nanotubes for the development of antimicrobial nanocomposites. Adv Colloid Interfac 275:102063
39. Sang B, Li ZW, Li XH, Yu LG, Zhang ZJ (2016) Graphene–based flame retardants: a review. J Mater Sci 51(18):8271–8295
40. Tharmavaram M, Pandey G, Rawtani D (2018) Surface modified halloysite nanotubes: A flexible interface for biological, environmental and catalytic applications. Adv Colloid Interfac 261:82–101
41. Wang Y, Wang W, Xu R, Zhu M, Yu D (2019) Flexible, durable and thermal conducting thiol–modified rGO–WPU/cotton fabric for robust electromagnetic interference shielding. Chem Eng J 360:817–828
42. Wang J, He J, Ma L, Zhang Y, Shen L, Xiong S, Li K, Qu M (2020a) Multifunctional conductive cellulose fabric with flexibility, superamphiphobicity and flame–retardancy for all–weather wearable smart electronic textiles and high–temperature warning device. Chem Eng J 390:124508
43. Wang B, Xu YJ, Li P, Zhang FQ, Liu Y, Zhu P (2020b) Flame–retardant polyester/cotton blend with phosphorus/nitrogen/silicon–containing nano–coating by layer–by–layer assembly. Appl Surf Sci 509:145323
44. Wang YL, Li ZP, Li YY, Wang JY, Liu X, Song TY, Yang XM, Hao JW (2018) Spray–drying–assisted layer–by–layer assembly of alginate, 3–aminopropyltriethoxysilane, and magnesium hydroxide flame retardant and its catalytic graphitization in ethylene–vinyl acetate resin. ACS Appl Mater Interfaces 10(12):10490–10500
45. Wu XN, Qian XR, An XH (2013) Flame retardancy of polyaniline–deposited paper composites prepared via in situ polymerization. Carbohydr Polym 92(1):435–440
46. Xue CH, Wu Y, Guo XJ, Liu BY, Wang HD, Jia ST (2020) Superhydrophobic, flame–retardant and conductive cotton fabrics via layer–by–layer assembly of carbon nanotubes for flexible sensing electronics. Cellulose 27(6):3455–3468
47. Xie H, Lai X, Li H, Gao J, Zeng X, Huang X, Zhang S (2020) A sandwich–like flame retardant nanocoating for supersensitive fire–warning. Chem Eng J 382:122929

48. Yuan BH, Wang BB, Hu YX, Mu XW, Hong NN, Liew KM, Hu Y (2016) Electrical conductive and graphitizable polymer nanofibers grafted on graphene nanosheets: Improving electrical conductivity and flame retardancy of polypropylene. Compos Part A–Appl S 84:76–86
49. Zhang Y, Tian WX, Liu LX, Cheng WH, Wang W, Liew KM, Wang BB, Hu Y (2019) Eco–friendly flame retardant and electromagnetic interference shielding cotton fabrics with multi–layered coatings. Chem Eng J 372:1077–1090
50. Zhang JJ, Chen B, Liu J, Zhu P, Liu Y, Jiang ZM, Dong CH, Lu Z (2020) Multifunctional antimicrobial and flame retardant cotton fabrics modified with a novel N,N–di(ethyl phosphate) biguanide. Cellulose 27(12):7255–7269
51. Zhao YT, Wang J, Li ZQ, Zhang XW, Tian MW, Zhang XS, Liu XQ, Qu J, Zhu SF (2020) Washable, durable and flame retardant conductive textiles based on reduced graphene oxide modification. Cellulose 27(3):1763–1771
52. Zhao L, Yan HQ, Fang ZP, Wang J, Wang H (2015) On the flameproof treatment of ramie fabrics using a spray–assisted layer–by–layer technique. Polym Degrad Stab 121:11–17
53. Zarrintaj P, Yazdi MK, Vahabi H, Moghadam PN, Saeb MR (2019)) Towards advanced flame retardant organic coatings: Expecting a new function from polyaniline. Prog Org Coat 130:144–148
54. Zeng FX, Qin ZY, Li T, Chen YY, Yang LF (2020) Boosting phosphorus–nitrogen–silicon synergism through introducing graphene nanobrick wall structure for fabricating multifunctional cotton fabric by spray assisted layer–by–layer assembly. Cellulose 27(11):6691–6705
55. Zeng FX, Qin ZY, Liang BL, Li T, Liu N, Zhu MF (2015) Polyaniline nanostructures tuning with oxidants in interfacial polymerization system. Prog Nat Sci: Mater Int 25(5):512–519
56. Zhou QQ, Chen JY, Zhou TC, Shao JZ (2020) In situ polymerization of polyaniline on cotton fabrics with phytic acid as a novel efficient dopant for flame retardancy and conductivity switching. New J Chem 44(8):3504–3513

Figures

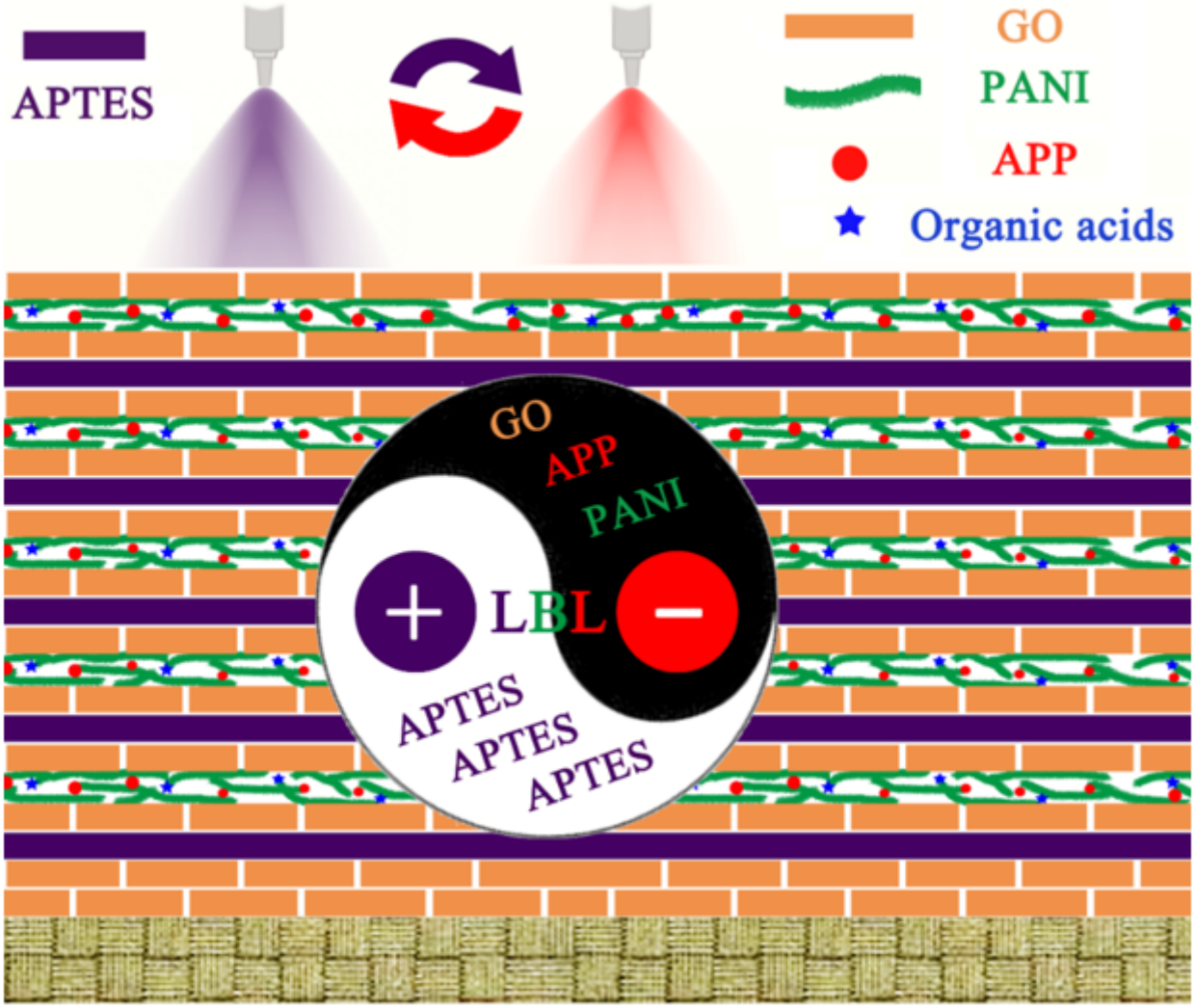

Figure 1

The fabrication and structural illustration for multifunctional CFs through spray–assisted LBL assembly.

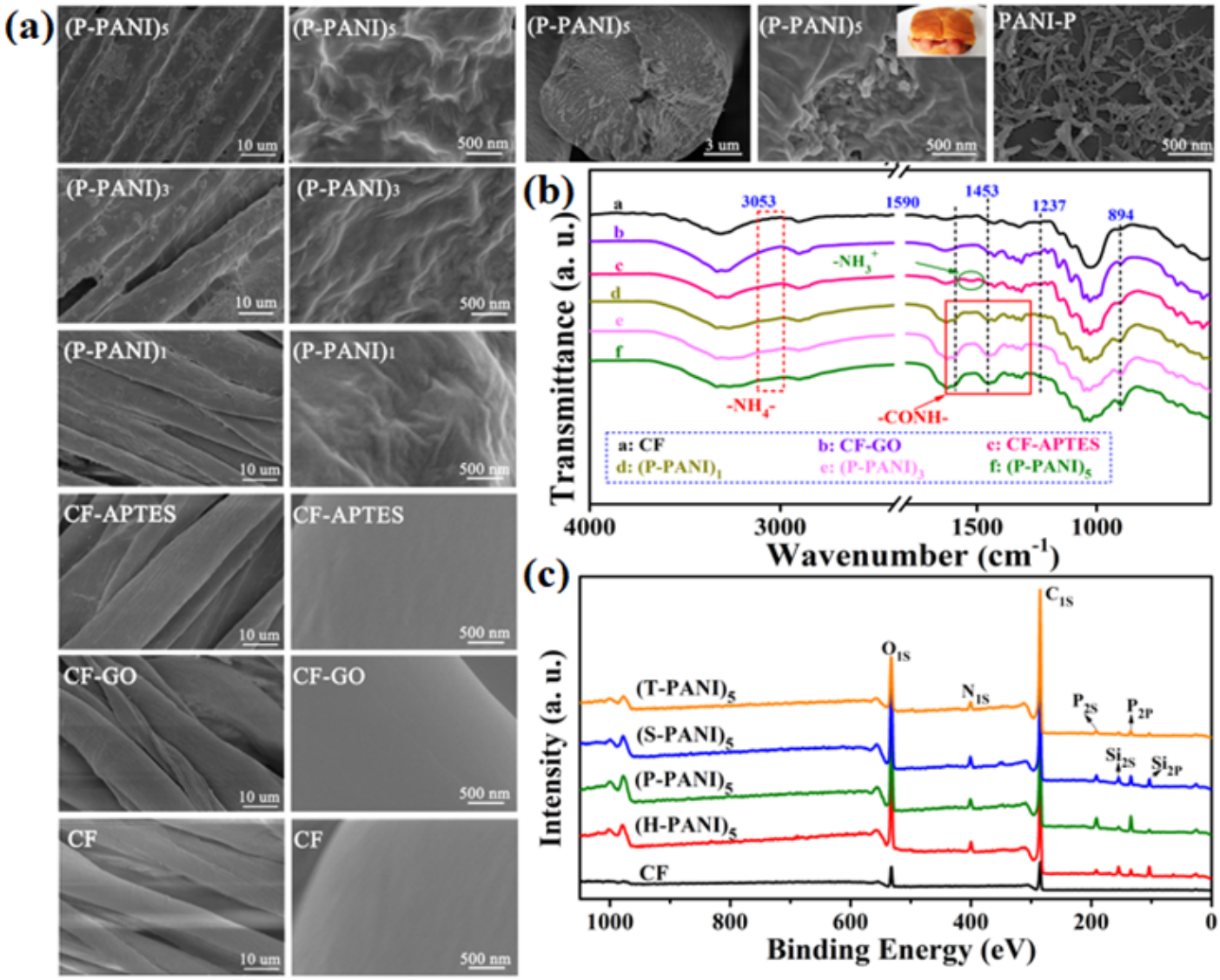

Figure 2

(a) Surface morphologies of neat CF and coated fabrics with GO, APTES, and different assembled layers, the section images of (P–PANI)5 as well as morphology of PANI–P; the insert gives photographic picture of the hot–dog; (b) ATR–FTIR spectra and (c) XPS patterns for neat CFs before and after coating.

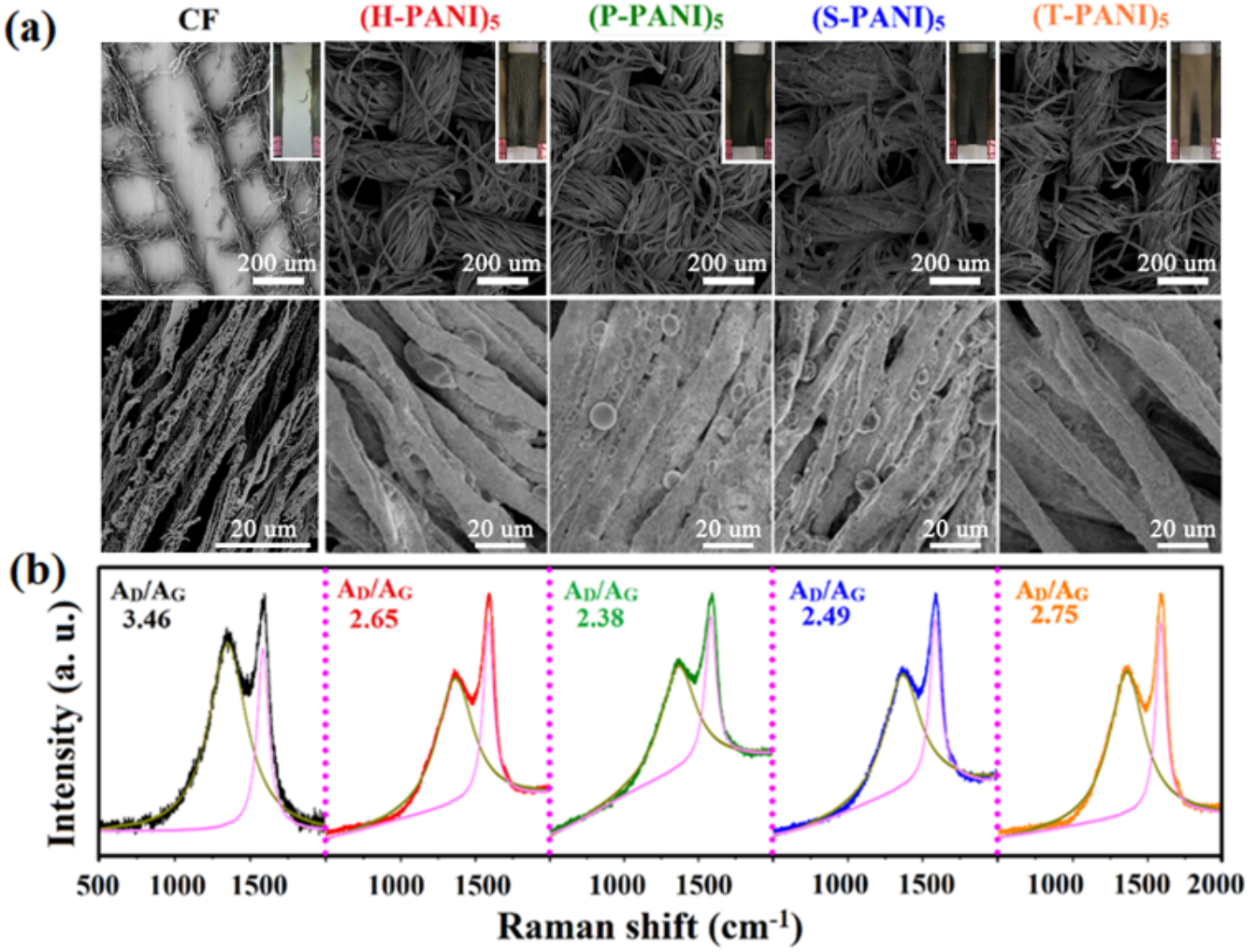

Figure 3

(a) Low and high magnification SEM images and (b) Raman spectra of the char residues after vertical flame test. The insert presents in situ photographs of vertical flame tests for neat CF and coated fabrics containing PANI nanofibers doped by different organic acids.

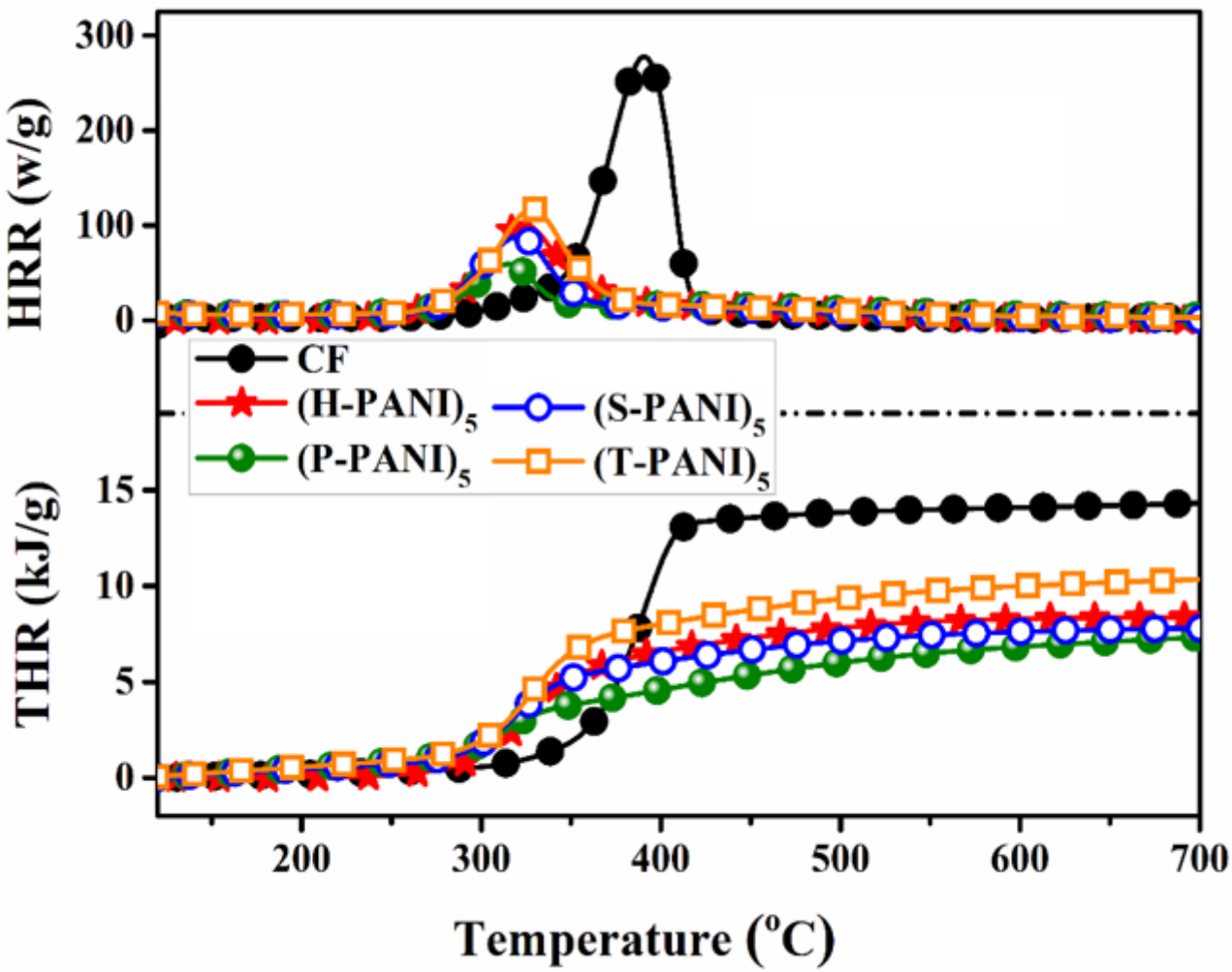

Figure 4

Heat release rate and total heat release curves as a function of temperature for neat CF and coated fabrics with PANI nanofibers doped by various organic acids.

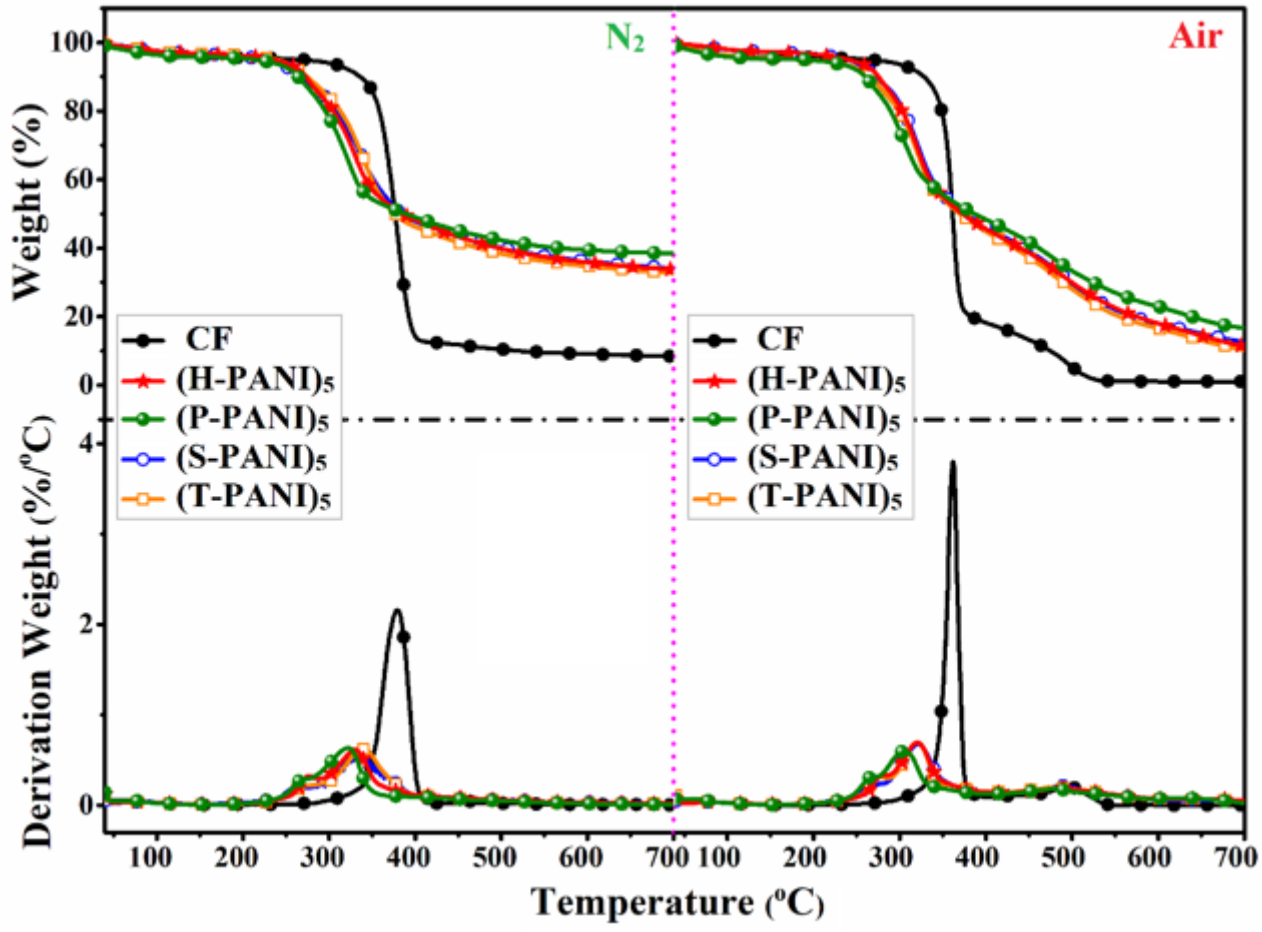

Figure 5

TGA and DTG curves for neat CF and coated fabrics under nitrogen and air atmospheres.

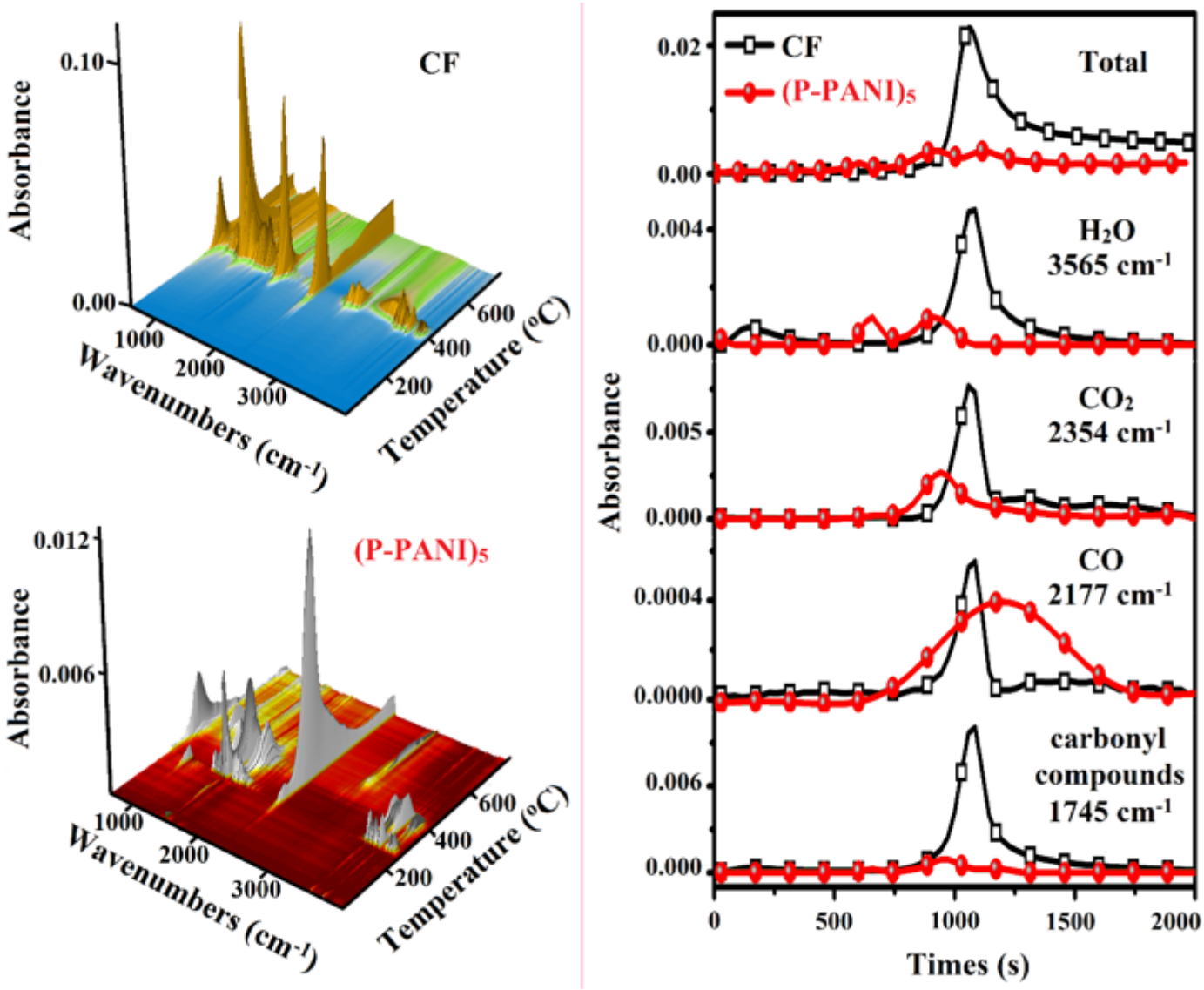

Figure 6

3D TG–IR spectra (left) and the absorbance of some pyrolysis products (right) for neat CF and (P–PANI)5.

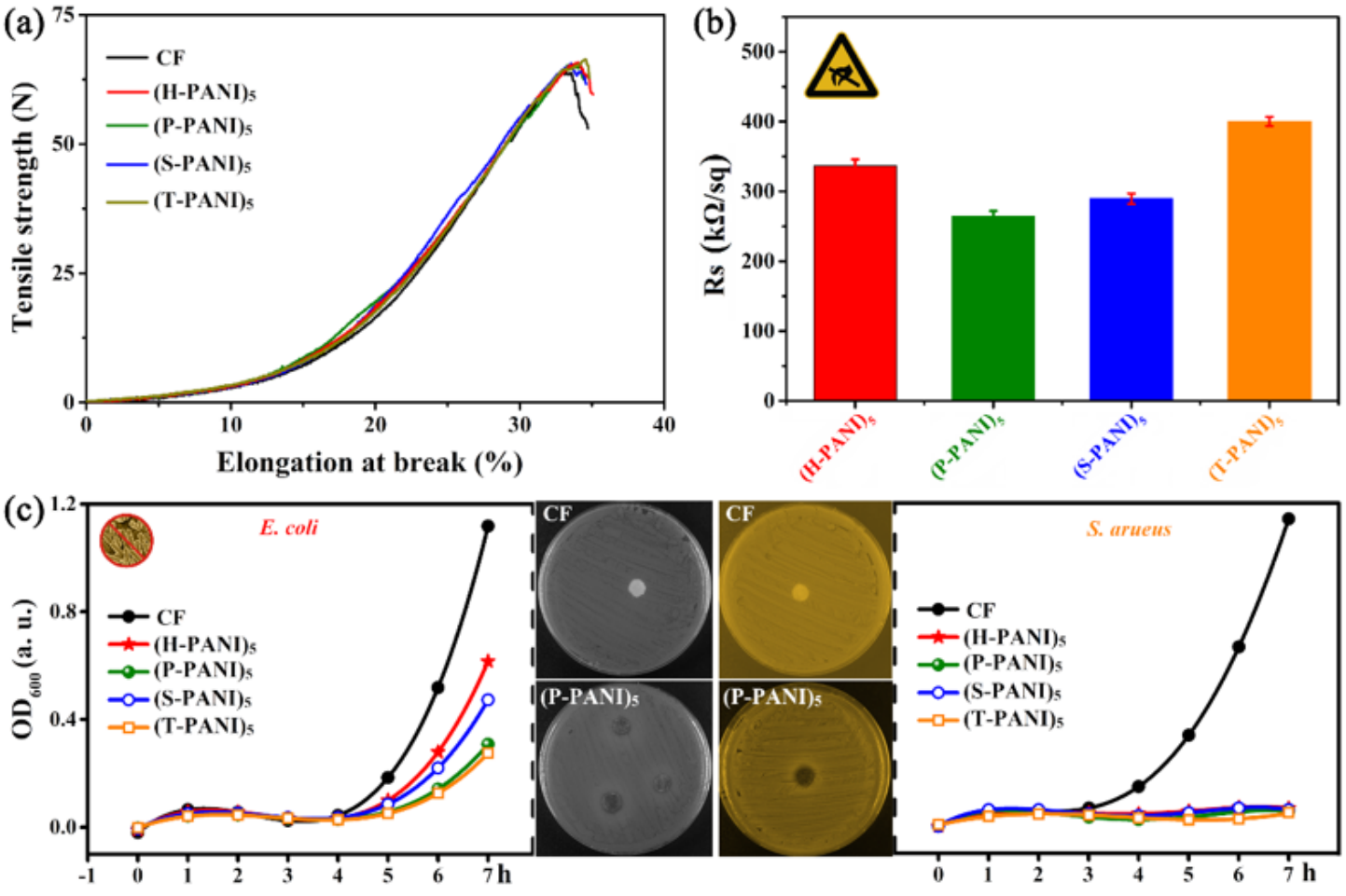

Figure 7

(a) The stress–strain curves, (b) sheet resistance and (c) antibacterial activity for neat CF and coated fabrics.

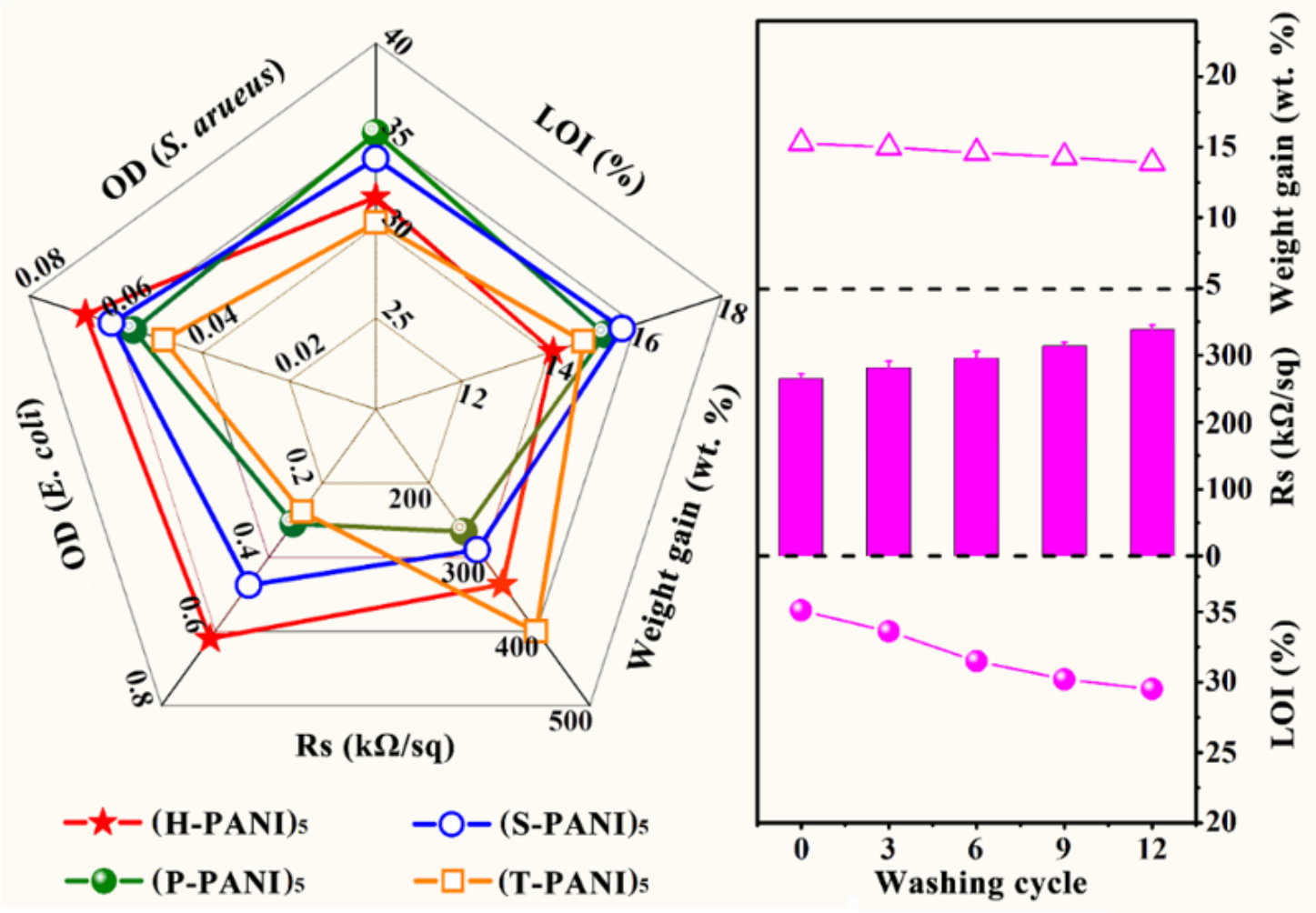

Figure 8

Performance comparison of all the coated fabrics at the same number of assembled layers (left) as well as plots of the weight gain, Rs and LOI value for (P–PANI)5 as a function of the number of washing cycles (right).

Supplementary Files

This is a list of supplementary files associated with this preprint. Click to download.

- graphicalabstract.png
- Supplementarydata.docx